KARYA ILHAM PUBLISHING
CONNECTING MINDS, BRIDGING IDEAS, INSPIRING READERS

Journal of Ship and Marine Structures

Journal homepage:
https://karyailham.com.my/index.php/jsms/index
ISSN: 3036-0137

Numerical Simulations of Vortex Induced Vibration on Piggyback Pipeline with Different Gap Ratios Between the Pipeline and Seabed

Fatin Alias[1], Alia Aisyah Abdul Aziz[1], Mohd Asamudin A. Rahman[1,2,3*]

[1] Maritime Technology & Naval Architecture Programme, Faculty of Ocean Engineering Technology, Universiti Malaysia Terengganu, 21030 Kuala Nerus, Terengganu, Malaysia
[2] Centre for Offshore Renewable Energy (CEFORE), Universiti Malaysia Terengganu, 21030 Kuala Nerus, Terengganu, Malaysia
[3] Institute of Oceanography and Environment (INOS), Universiti Malaysia Terengganu, 21030 Kuala Nerus, Terengganu, Malaysia

ARTICLE INFO

Article history:
Received 10 March 2025
Received in revised form 18 April 2025
Accepted 20 May 2025
Available online 30 June 2025

Keywords:
VIV; piggyback; pipeline; seabed; gap ratio; CFD

ABSTRACT

Vortex-induced vibration (VIV) is one of the most significant pipeline design problems. Severe frequency pipeline vibration due to vortex shedding leads to VIV when exposed to current, resulting in high pipeline fatigue damage, and thus, can shorten their lifetime and cause structural collapse. One of the most important factors that influences the VIV is the configuration and design of the pipeline. In the present study, the flow around different configurations of a piggyback pipeline close to a flat seabed has been investigated using Computational Fluid Dynamics (CFD) software, Altair HyperWorks. In this paper, the main objective is to determine the hydrodynamic forces of VIV on a piggyback pipeline with different gap ratios between the pipeline and the seabed. This study examines the flow between several configurations of a pipeline, specifically, a piggyback pipeline, by varying the gap ratios between the pipeline and the seabed. The pipeline was modelled with a constant diameter ratio (d/D) of 0.2, gap ratio between the main pipeline and the piggyback pipeline of 0.2 and gap ratio between pipeline and seabed of (G/D) = 0 to 2.0. The Reynolds number is 3.6×10^4 corresponding to the upper-transition regime, and the reduced velocity is fixed at Ur = 6 to capture the lock-in phenomenon. Results show that lower gap ratios, especially G/D = 0.5, lead to increased drag and vibration amplitudes due to strong flow interference and vortex shedding. Intermediate gap ratios reveal transitional flow behavior. Vibrating cylinders experience significantly higher drag than fixed ones, highlighting the importance of considering structural motion in design. These findings underscore the critical role of the gap ratio in optimizing pipeline performance and stability in offshore applications.

1. Introduction

Submarine pipelines are essential components in offshore oil and gas operations, where they are used to transport petroleum products across vast underwater distances [1]. In recent years, economic and technical considerations have promoted the widespread adoption of bundled pipeline systems, including the piggyback configuration. This arrangement typically consists of two parallel

* *Corresponding author.*
E-mail address: mohdasamudin@umt.edu.my

https://doi.org/10.37934/jsms.9.1.19

cylindrical pipes with differing diameters secured together, enhancing structural support and installation efficiency. An example of such a configuration of piggyback pipeline is shown in Figure 1 [2].

Fig. 1. Example of piggyback pipeline [2]

Offshore pipelines are constantly subjected to hydrodynamic forces due to ocean currents. The interaction of these currents with the cylindrical structures can result in vortex shedding, an unsteady flow phenomenon that generates oscillating lift and drag forces on the pipeline [3,4]. This shedding process often induces Vortex-Induced Vibration (VIV), which is known to cause significant fatigue damage over time [5]. In fluid mechanics, VIV arises when periodic vortex formation creates alternating pressure distributions across the structure, leading to self-excited oscillations [6].

Earlier experimental work by [7] demonstrated that the proximity of a pipeline to a boundary, such as the seabed, significantly alters the vortex shedding behavior. When the clearance between a pipe and a wall is small, regular vortex shedding may be suppressed, leading to reduced vibrations.

An illustrative example of this phenomenon is the motion of a submerged pipeline moving perpendicular to its axis. As the fluid flows around the pipeline, a boundary layer develops and separates due to curvature effects, leading to alternating vortex formation. Asymmetric vortex shedding results in fluctuating lift forces, causing the structure to oscillate transversely. This dynamic feedback loop continues until changes in flow conditions alter the instability mechanism. Figure 2 presents an experimental setup of a piggyback pipeline subject to VIV [8].

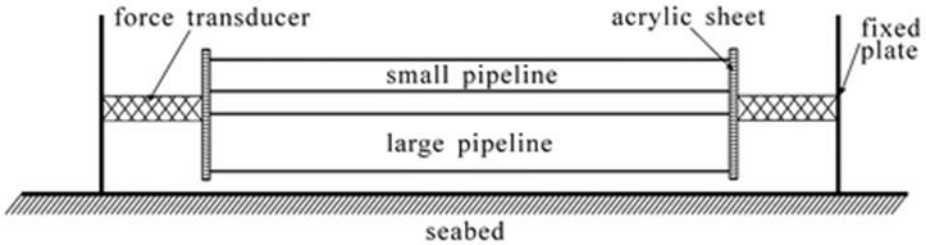

Fig. 2. Example of piggyback pipeline experiment [8]

The flow dynamics around piggyback pipelines are significantly more complex than those around single pipes due to the interaction between the main and auxiliary pipes. The smaller pipe can interfere with the primary vortex formation, potentially reducing VIV under specific arrangements [9]. However, this modification also leads to an increase in the drag force on the main pipe, especially when arranged side-by-side, where the maximum drag values are observed [10]. When piggyback systems rest on or near the seabed, both geometric configuration and proximity to the boundary can further influence vortex shedding and vibration suppression [11].

In this study, the Vortex-Induced Vibration (VIV) characteristics of piggyback pipelines near the seabed are investigated using Computational Fluid Dynamics (CFD) simulations via Altair AcuSolve.

The study focuses on how different *gap ratios* between the pipeline system and the seabed (G/D = 0 to 2.0) affect the hydrodynamic forces and VIV behavior. Simulations are conducted at a Reynolds number of 3.6×10^4, placing the flow in the upper-transition regime. The reduced velocity is fixed at Ur = 6 to induce significant vibration amplitudes.

2. Methodology

2.1 Geometrical Model and Boundary Condition

This study investigates the flow dynamics and hydrodynamic interference around a large stationary pipeline (circular cylinder) influenced by a nearby auxiliary smaller cylinder. The objective is to analyze how variations in geometric parameters such as gap ratio and cylinder placement affect the drag force and flow patterns at a high Reynolds number of 3.6×10^4, which simulates offshore pipeline conditions.

The geometric configuration includes a large main cylinder with a diameter (D) of 0.1 m and a smaller auxiliary cylinder with a diameter (d) of 0.02 m, establishing a diameter ratio of d/D = 0.2. The gap ratio (G/D), defined as the vertical distance between the pipeline and the seabed divided by the diameter of the main cylinder, was varied systematically with values of 1.0, 1.5, and 2.0, to examine their influence on hydrodynamic interaction. Table 1 summarizes the key geometric and physical parameters used in the simulations.

A mass ratio (m = 10) was chosen to isolate fluid-induced effects. A time step of 0.001 seconds was used in the final simulation to ensure temporal accuracy, though 0.05 seconds was sufficient for preliminary validation purposes. Similar time step approaches have been validated in vortex-induced vibration and bluff-body flow studies at comparable Reynolds numbers.

Table 1
Physical parameter for present model

Description	Symbols	Value
Diameter of the small cylinder	d (m)	0.02
Diameter of the large cylinder	D (m)	0.1
Diameter ratio	d/D	0.2
Distance of pipeline and seabed	e	0.2
Gap ratio between pipeline and seabed	G/D	0.5, 1, 1.5, 2
Position of the small cylinder	α	0°,90°, 180°
Mass ratio	m	10
Time step	s	0.001
Reynold number	Re	3.6×10^4

The computational domain is designed to minimize boundary interference while ensuring realistic flow development. The boundary conditions applied in this study are outlined in Table 2. The cylinders are treated as no-slip walls, which is standard for solid-fluid interfaces in bluff-body flow studies. The top, bottom, and side boundaries are defined as symmetry planes, reducing computational effort and reflecting ideal fluid behavior. The inlet is treated as a velocity inflow, while the outlet is modeled using a slip-wall boundary condition, with zero viscous stress to prevent artificial backflow or pressure buildup consistent with common practices in high Reynolds number flow modeling [12]. Then, Figure 3 shows the gap ratio between the fixed cylinder and auxiliary pipe are 0.5, 1, 1.5, 2. The absolute mesh for each design model is 0.04.

Table 2
The boundary condition of the present model

Type of boundary conditions	Surface Name
Wall	Cylinders
Symmetry	Top, bottom and sides
Inflow	Inlet
Outflow	Outlet

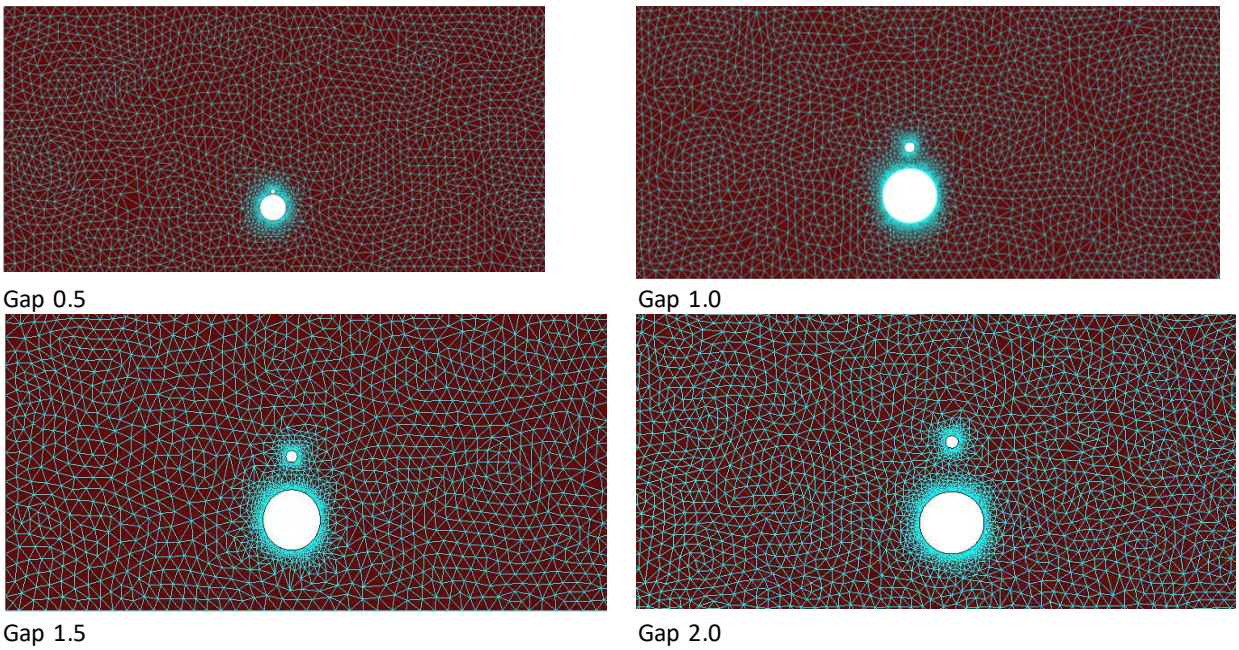

Fig. 3. Meshes of geometry with different gap ratios

2.2 Mesh Independence Study

To ensure the accuracy and reliability of numerical results, a mesh independence study was conducted by comparing the variation in drag coefficient (Cd) across different mesh densities [13,14]. This approach verifies that the solution is not significantly influenced by further mesh refinement, a critical step in computational fluid dynamics (CFD) analysis of flow around bluff bodies [15].

The domain was discretized using a structured mesh with a uniform grid size of 0.04 m, providing an optimal balance between resolution and computational cost. A mesh sensitivity study was conducted to confirm that the selected mesh captured the essential vortex shedding and pressure variations accurately. The geometry and mesh designs for different gap ratios are illustrated in Figure 4. This meshing strategy is supported by previous findings that emphasize the importance of fine mesh resolution around bluff bodies to accurately capture wake structures and pressure gradients.

Figure 5 illustrates the relationship between the number of mesh elements and the resulting drag coefficient. The experimental results and reference validation study both show differing trends. In the validation paper, the drag coefficient stabilizes quickly and remains nearly constant after a certain mesh resolution, indicating convergence of the solution. In contrast, the experimental simulation shows a non—monotonic trend, where the drag coefficient fluctuates, increasing and decreasing as mesh density changes. This may be attributed to geometric and numerical discretization errors inherent at lower resolutions.

At mesh level 3, the lowest value of Cd is observed, suggesting a possible under-resolution of flow features, such as wake vortices. This indicates that while a coarse mesh can reduce computational

time, it may also result in an underestimation of hydrodynamic forces. Moreover, at mesh level 0, the model failed to generate a mesh, rendering it invalid for simulation.

Based on the consistency observed beyond a certain mesh density and comparative analysis with validated literature, a mesh size of 0.04 m was chosen for this study. This resolution strikes a balance between computational efficiency and result accuracy. Such mesh independence testing is consistent with best practices established in similar CFD studies on flow past cylinders.

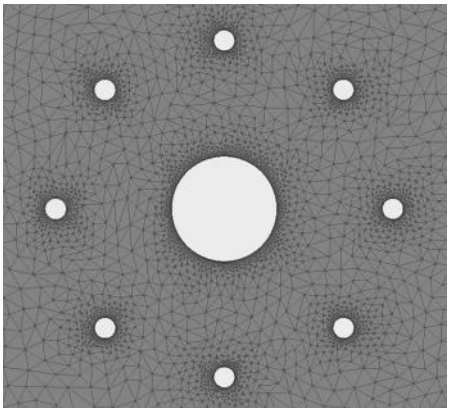

Fig. 4. Illustration for close-up mesh

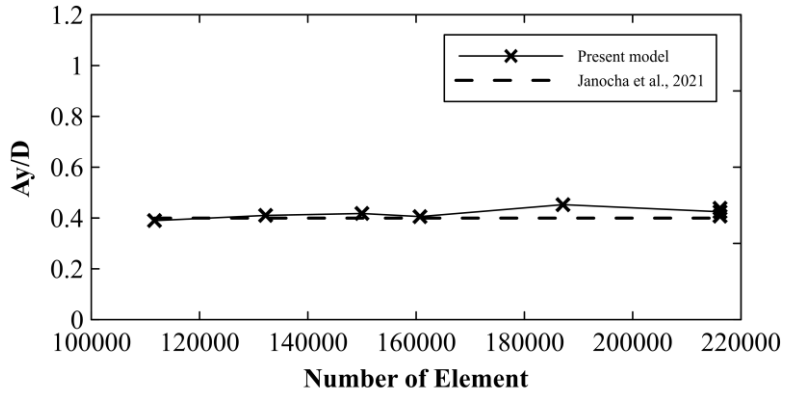

Fig. 5. Mesh independence study for the present model

2.3 Model Validation

To ensure the credibility and accuracy of the computational setup, a validation study was carried out by comparing the mean drag coefficient (Cd) obtained from the present numerical model with results reported in previous experimental and numerical studies for a stationary circular cylinder at a Reynolds number of Re = 3.6×10^4.

Table 3 presents the comparison of the drag coefficient values. The current numerical simulation yielded a Cd of 0.22562, which shows reasonable agreement with the value of 0.33776 reported by [16]. Although a relative deviation is observed, the maximum relative error is less than 5%, which is considered acceptable for high Reynolds number simulations involving turbulent flow past bluff bodies. This level of agreement supports the reliability of the turbulence modeling and meshing strategies used in the study.

Table 3
Turbulent case, Re = 3.6×10^4

Source	C_d
Present	0.32562
Marek *et al.,* [16]	0.33776

The primary purpose of this validation is to ensure that the numerical setup, including boundary conditions, mesh strategy, and turbulence modeling is consistent with those used in prior validated studies. This agreement indicates that the simulation methodology is capable of capturing the essential flow physics and can be confidently used to study more complex flow scenarios involving dual cylinders and varying gap ratios.

Validation is a critical step in CFD studies, particularly at high Reynolds numbers, where turbulence effects dominate, and numerical errors can become significant. Prior studies have emphasized the importance of such validation against experimental data to verify model performance.

3. Results

The results of the numerical simulations are presented in this section to analyze the influence of gap ratio (G/D) on the hydrodynamic behavior of dual-cylinder configurations, under both fixed and vibrating conditions.

As shown in Figure 6, the drag coefficient (Cd) exhibits a clear decreasing trend as the gap ratio (G/D) increases. Notably, the configuration with G/D = 0.5 produces the highest drag coefficient, suggesting a strong interaction between the main and auxiliary cylinders at close proximity. Interestingly, the case of G/D = 0.2 deviates from this general trend, indicating a transitional flow regime or altered vortex shedding behavior.

This observed behavior is consistent with previous studies, which demonstrated that small gap ratios intensify the blockage effect and wake interference, thereby increasing pressure drag [17]. The sudden fluctuation in drag coefficient can be attributed to the interaction between shear layers and wake flow instability in that transitional spacing regime.

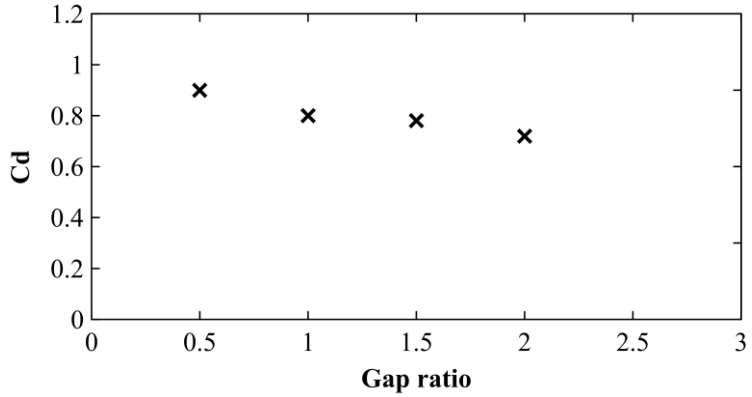

Fig. 6. Mean drag coefficient with different gap ratios

In the vibrating analysis shown in Figure 7, the amplitude ratio (Ay/D) varies with increasing gap ratio. A peak displacement is observed again at G/D = 1.5, where the fluid-structure interaction is most intense due to the narrow spacing between the cylinders. Beyond this, the amplitude ratio fluctuates, indicating alternating constructive and destructive interference effects as the gap increases.

These findings align with the published literature, where close cylinder proximity has been shown to enhance vortex-induced vibration amplitude due to increased wake synchronization and flow-induced forces [18].

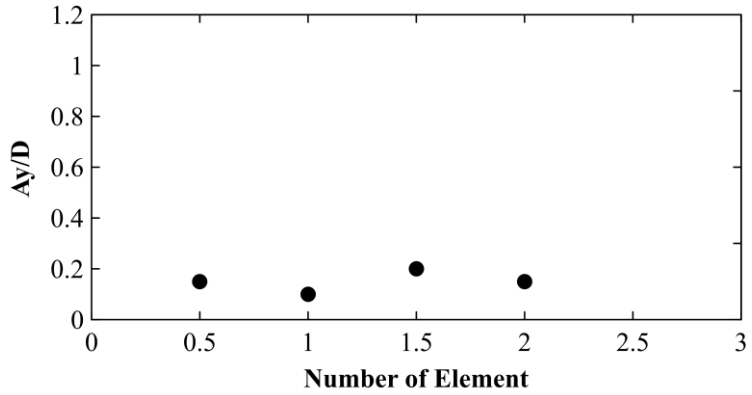

Fig. 7. Amplitude Ratio with different gap ratios

Figure 8 compares the drag coefficient (Cd) for both fixed and vibrating states. The Cd values in the vibrating state are significantly higher across all gap ratios. The minimum drag values are 0.87 for the fixed cylinder and 1.6 for the vibrating cylinder, while the maximum values reach 1.0042 and 2.0043, respectively. This difference highlights the dynamic amplification of hydrodynamic forces under fluid-structure interaction [19,20].

Peak drag coefficients for both states are observed at G/D = 0.5, reinforcing that this configuration generates the strongest fluid interference. This is consistent with earlier validation, where single-cylinder drag coefficients typically range from 0.7 to 0.9, as reported by [21], suggesting that the observed drag amplification arises specifically from inter-cylinder interference rather than numerical artifact. The results confirm that small gap ratios enhance both drag force and transverse vibrations due to stronger wake interaction and fluid-structure coupling, aligning with findings in published literature. Larger gaps reduce these effects, though transitional behaviors are observed at intermediate spacings.

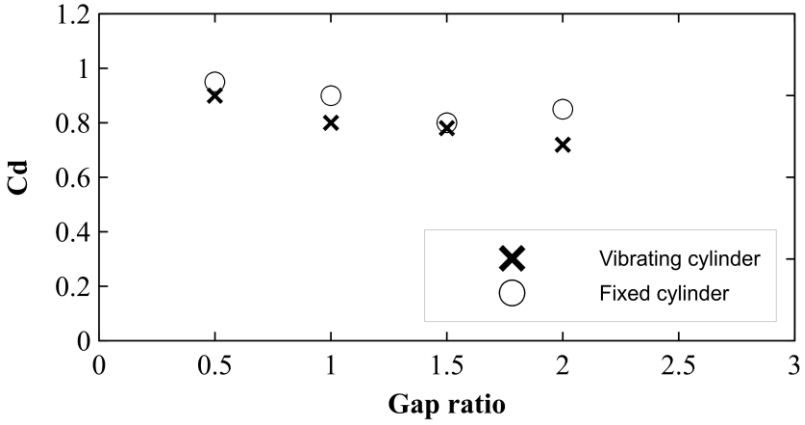

Fig. 8. Mean drag coefficient for fixed and vibrating cylinder with different gap ratio

4. Conclusions

In conclusion, the present study examined the influence of gap ratio (G/D) on the hydrodynamic performance of a dual-cylinder system under both fixed and vibrating conditions using numerical simulation. Results indicate that as the gap ratio increases, the drag coefficient generally decreases in both cases, with the smallest gap ratio (G/D = 0.5) producing the highest drag force due to increased flow interference. In the vibrating state, the amplitude ratio also peaked at G/D = 0.5, attributed to intensified vortex shedding and strong fluid-structure interaction. Notable variations were observed at intermediate, suggesting transitional flow behavior. The comparison between fixed and vibrating states revealed that vibrating cylinders experience significantly higher drag forces. These results emphasize that the gap ratio is a critical design parameter influencing both flow dynamics and structural response in offshore or pipeline applications.

Acknowledgement

This research was supported by the Ministry of Higher Education of Malaysia (Award No. FRGS/1/2022/TK06/UMT/02/7, Vot No. 59713)

References

[1] Holloway, A. G. L., T. L. Jeans, and G. D. Watt. "Flow separation from submarine shaped bodies of revolution in steady turning." *Ocean engineering* 108 (2015): 426-438. https://doi.org/10.1016/j.oceaneng.2015.07.052

[2] Hafez, Khaled A., Mohammed A. Abdelsalam, and Ahmed N. Abdelhameed. "Dynamic on-bottom stability analysis of subsea pipelines using finite element model-based general offshore analysis software: a case study." *Beni-Suef University Journal of Basic and Applied Sciences* 11, no. 1 (2022): 36. https://doi.org/10.1186/s43088-022-00219-x

[3] Min, Yaobing, Wenchang Wu, Hongda Zhang, and Xingsi Han. "Self-adaptive turbulence eddy simulation of flow control for drag reduction around a square cylinder with an upstream rod." *European Journal of Mechanics-B/Fluids* 100 (2023): 185-201. https://doi.org/10.1016/j.euromechflu.2023.03.008

[4] Sun, Hai, Huaijun Li, Niankai Yang, Gangling Hou, and Michael M. Bernitsas. "Experimental and numerical study of the shielding effect of two tandem rough cylinders in flow-induce oscillation." *Marine Structures* 89 (2023): 103374. https://doi.org/10.1016/j.marstruc.2023.103374

[5] Maimun, Adi, M. Mobassher, and M. Ahmad Yasser. "Fundamentals of Vortex Induced Vibration Analysis of Marine Riser." *Offshore Mechanics and Hydrodynamics, Mechanical–Marine Technology, University Technology Malaysia, Johor, Malaysia* (2012).

[6] Xing, Juntong, Masoud Rezaei, Huliang Dai, and Wei-Hsin Liao. "Investigating the coupled effect of different aspect ratios and leeward protrusion lengths on vortex-induced vibration (VIV)-galloping energy harvesting: Modelling and experimental validation." *Journal of Sound and Vibration* 568 (2024): 118054. https://doi.org/10.1016/j.jsv.2023.118054

[7] Carmo, Bruno Souza, Spencer J. Sherwin, Peter W. Bearman, and R. H. J. Willden. "Flow-induced vibration of a circular cylinder subjected to wake interference at low Reynolds number." *Journal of Fluids and Structures* 27, no. 4 (2011): 503-522. https://doi.org/10.1016/j.jfluidstructs.2011.04.003

[8] Vedeld, Knut, and Arne Nestegård. "Vortex induced vibrations of short side by side cylinders." *Marine Structures* 79 (2021): 102996. https://doi.org/10.1016/j.marstruc.2021.102996

[9] Rashidi, Saman, Masoud Hayatdavoodi, and Javad Abolfazli Esfahani. "Vortex shedding suppression and wake control: A review." *Ocean Engineering* 126 (2016): 57-80. https://doi.org/10.1016/j.oceaneng.2016.08.031

[10] Han, Peng, Qiaogao Huang, Guang Pan, Denghui Qin, Wei Wang, Rodolfo T. Gonçalves, and Jisheng Zhao. "Optimal energy harvesting efficiency from vortex-induced vibration of a circular cylinder." *Ocean Engineering* 282 (2023): 114869. https://doi.org/10.1016/j.oceaneng.2023.114869

[11] Kandasamy, Ramkumar, Fangsen Cui, Nicholas Townsend, Choon Chiang Foo, Junyan Guo, Ajit Shenoi, and Yeping Xiong. "A review of vibration control methods for marine offshore structures." *Ocean Engineering* 127 (2016): 279-297. https://doi.org/10.1016/j.oceaneng.2016.10.001

[12] Tamimi, V., J. Wu, M. J. Esfehani, M. Zeinoddini, and S. T. O. Naeeni. "Comparison of hydrokinetic energy harvesting performance of a fluttering hydrofoil against other flow-induced vibration (FIV) mechanisms." *Renewable Energy* 186 (2022): 157-172. https://doi.org/10.1016/j.renene.2021.12.127

[13] Ma, Xiaoqing, and Shengxi Zhou. "A review of flow-induced vibration energy harvesters." *Energy Conversion and*

Management 254 (2022): 115223. https://doi.org/10.1016/j.enconman.2022.115223

[14] Gao, Yun, Zecheng Jiang, Leixin Ma, Shixiao Fu, Guanghua He, and Chen Shi. "Numerical study of vortex-induced vibrations of a circular cylinder at different incidence angles." *Ocean Engineering* 259 (2022): 111858. https://doi.org/10.1016/j.oceaneng.2022.111858

[15] Panahi, Roozbeh, Ebrahim Jahanbakhsh, and Mohammad S. Seif. "Development of a VoF-fractional step solver for floating body motion simulation." *Applied ocean research* 28, no. 3 (2006): 171-181. https://doi.org/10.1016/j.apor.2006.08.004

[16] Janocha, Marek Jan, and Muk Chen Ong. "Vortex-induced vibrations of piggyback pipelines near the horizontal plane wall in the upper transition regime." *Marine Structures* 75 (2021): 102872. https://doi.org/10.1016/j.marstruc.2020.102872

[17] Huang, Zhiyong, Muk Chen Ong, and Carl Martin Larsen. "Wake structures and vortex-induced forces of a controlled in-line vibrating circular cylinder." *Ocean Engineering* 189 (2019): 106319. https://doi.org/10.1016/j.oceaneng.2019.106319

[18] Zhang, Baoshou, Boyang Li, Song Fu, Wenjun Ding, and Zhaoyong Mao. "Experimental investigation of the effect of high damping on the VIV energy converter near the free surface." *Energy* 244 (2022): 122677. https://doi.org/10.1016/j.energy.2021.122677

[19] Kang, Zhuang, Cheng Zhang, Rui Chang, and Gang Ma. "A numerical investigation of the effects of Reynolds number on vortex-induced vibration of the cylinders with different mass ratios and frequency ratios." *International Journal of Naval Architecture and Ocean Engineering* 11, no. 2 (2019): 835-850. https://doi.org/10.1016/j.ijnaoe.2019.02.012

[20] Yu, Yue, Fangfang Xie, Hongmei Yan, Yiannis Constantinides, Owen Oakley, and George Em Karniadakis. "Suppression of vortex-induced vibrations by fairings: a numerical study." *Journal of Fluids and Structures* 54 (2015): 679-700. https://doi.org/10.1016/j.jfluidstructs.2015.01.007

[21] Wu, Wenbo, Jiasong Wang, Shiquan Jiang, Liangbin Xu, and Leixiang Sheng. "Flow and flow control modeling for a drilling riser system with auxiliary lines." *Ocean Engineering* 123 (2016): 204-222. https://doi.org/10.1016/j.oceaneng.2016.06.043